STUDY AND DEVELOPMENT OF A SOLAR RADIATION PREDICTING ALGORITHM BASED ON ECMWF'S FORECASTS AND ANNS

Sara Pereira[1], Paulo Canhoto[1], Rui Salgado[1] and Maria João Costa[1]

[1]Institute of Earth Sciences, University of Évora, 7000-671 Portugal

This paper presents a study on the influence of Sun-Earth geometry and atmospheric variables on the predictions of solar global irradiation (GHI) obtained from the ECMWF model. It was found that the differences between predictions and measurements of GHI are correlated mainly with the clearness index, solar zenith angle, mean air temperature, relative humidity and total water column. An artificial neural network is developed to improve predictions of GHI for four locations being the base for a predicting algorithm that can be used in energy management models of solar systems thus allowing a better management of renewable energy conversion.

Keywords: solar radiation, solar energy, solar radiation forecast, ECMWF model, artificial neural network

INTRODUCTION

Weather forecast is a field of study that aims to predict the meteorological conditions based on physical laws and mathematical and numerical models that also incorporate observations made throughout the world, thus generating prognostic data. On the other hand, renewable energy resources like solar energy and wind power are particularly dependent on the weather conditions and so, weather forecast can be used to predict the energy output of systems converting such resources and adapt auxiliary power generating units or even the electric grid. The study presented here was conducted under a project whose goal is the development of a solar radiation forecast algorithm that produces half-hourly Global Horizontal Irradiation (GHI) and mean air temperature forecasts for a specific location in a time horizon of 72h, that will then be implemented in energy management models in medium/low temperature solar thermal systems.

The solar radiation that reaches the Earth's surface is affected by many factors such as the atmospheric components that absorb, reflect and/or scatter the solar radiation while it crosses the medium. In addition, the apparent Sun position as observed from the Earth's surface is also important since it influences the path crossed by the radiation in the atmosphere until it reaches the surface. Thus, studies of the influence of these variables on GHI predictions were conducted and an artificial neural network (ANN) was developed for the correction of these. ANNs are computing systems inspired by the biological neural networks that constitute animal brains using its fundamental cells, the neurons. Such systems progressively improve performance on tasks by considering examples, generally without task-specific programming [1]. ANNs have been used by many authors for correction of wind speed and daily solar irradiance forecasts, simulation of photovoltaic power using weather forecasts amongst others [2]–[9]. In this work, examples of using the developed ANN are presented showing how the predicted GHI values can be corrected taking as reference experimental values.

DATA

The data available for analysis and development of the algorithm are the hourly GHI predictions from the European Centre for Medium-range Weather Forecast (ECMWF) grid over Portugal with a 0.125×0.125° resolution [10] as well as the atmospheric variables of visibility, cloud base height, total column water, total cloud cover, 10 meter horizontal N-S and E-W wind components, air temperature and dewpoint temperature at 2 meters and total column ozone. The desired output of the algorithm is half-hourly GHI and mean air temperature predictions in a temporal horizon of 72 hours for a specific location. In a previous study [11], methods for temporal downscaling (from hourly values to half-hourly values) were developed and methods of spatial downscaling were studied resulting in the application of bi-linear interpolation on the nearest four points to the installation site. Reference measurements were obtained from ICT (Instituto de Ciências da Terra) stations located at Évora (CM6B Kipp & Zonen pyranometer 38.567687N 7.91704W), and Sines (Li-200R Li-COR pyranometer 37.9540833N 8.8654722W) with 1-minute time step of irradiance values, and from the IPMA (Instituto Português do Mar e da Atmosfera) stations at Cabo da Roca (38.781633N 9.497539W) and Penhas Douradas (40.411396N 7.558630W) (CM11 Kipp & Zonen pyranometers) with 1-hour values. The pyranometer located at Sines has lower precision [12] and is affected by shading during the first hour after sunrise. Experimental data from 13th May 2015 until 15th November 2016 in Évora and from 24th June 2015 until 15th November 2016 in Sines, Cabo da Roca and Penhas Douradas were used for the study. These measurements were then filtered and converted to hourly values of GHI (J/m^2). The comparison between predictions and measurements is made through absolute hourly differences between predictions and measurements.

INFLUENCE OF SUN-EARTH GEOMETRY AND ATMOSPHERIC VARIABLES

The analysis was made with the computed variables: zenith angle and clearness index (defined as the ratio between GHI and the hourly extraterrestrial irradiation) and the spatially downscaled ECMWF's hourly predictions of mean air temperature, air relative humidity (calculated using 2 meter air temperature and dewpoint temperature predictions), wind intensity (calculated using 10 meter horizontal N-S and E-W wind components), cloud cover fraction, cloud base height, total water column, total ozone column and visibility. Figures 1 and 2 show boxplots of the differences between predictions and measurements of GHI as a function of the clearness index (calculated using the predicted GHI data, since the final algorithm will not have access to measured data) for Évora and Sines, respectively. In the case of Évora, the model shows an underestimation of the solar global irradiation for values of clearness index below 45% and an overestimation of the solar global irradiation above this value. The same pattern is obsreved for Sines although the differences become positive for values of clearness index above 30%. It is also observed that the differences are generally higher for Sines than for Évora.

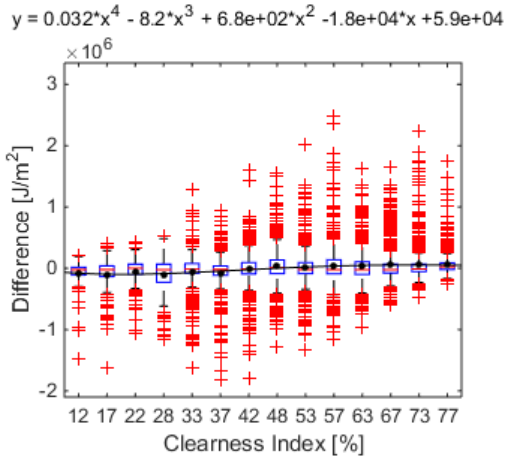

Fig. 1. Boxplot, mean values and polynomial function of hourly differences for each class of clearness index in Évora.

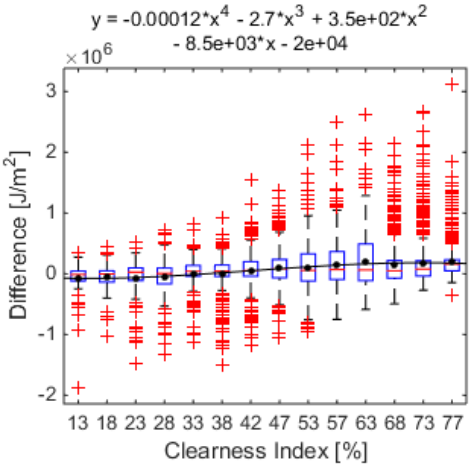

Fig. 2. Boxplot, mean values and polynomial function of hourly differences for each class of clearness index in Sines.

Figures 3 and 4 show the mean hourly differences between predicted and measured GHI data for each class of solar zenith angle and clearness index for Évora and Sines. The mean differences are higher for lower values of zenith angle which are characterized by higher values of GHI. However, these differences are not higher for higher values of clearness indexes (which are also characterized by higher values of GHI) but for values between approximately 40% and 70% when there are clouds that are difficult to forecast at shorter time scales.

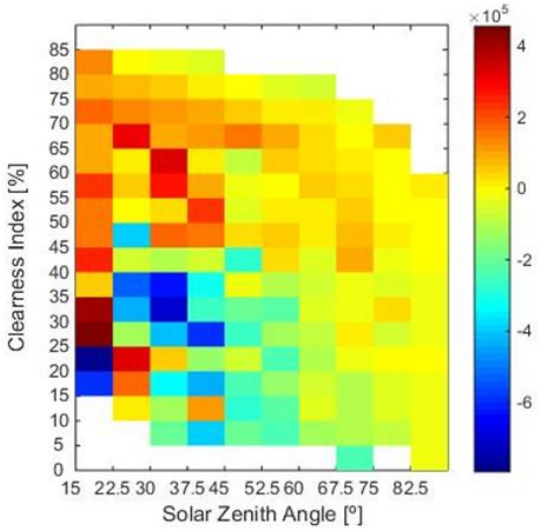

Fig. 3. Hourly difference mean (in J/m^2) for each class of solar zenith angle and clearness index in Évora.

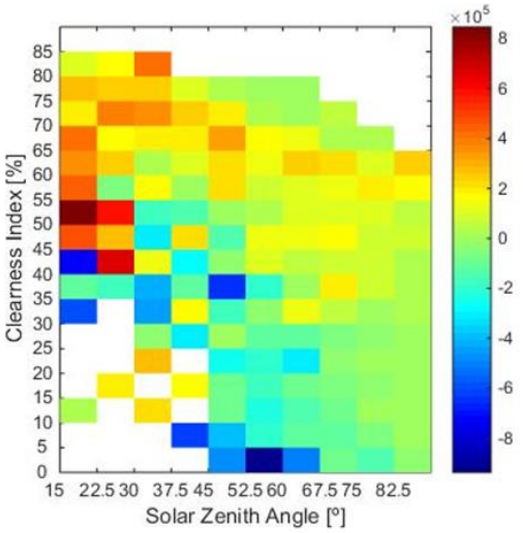

Fig. 4. Hourly difference mean (in J/m^2) for each class of solar zenith angle and clearness index in Sines.

The differences between predicted and measured values of GHI showed a relation with the predicted values of mean air temperature (higher differences for higher values of mean air temperature), relative humidity (higher differences for lower relative humidity values) and total water column (higher differences for higher values of total water column).

ANN DEVELOPMENT

After the previous analysis, the best parameters (architecture, input variables, training function, transfer function, data division type, number of neurons) for a corrective ANN using MATLAB's neural network toolbox were studied not only for the data from Évora and Sines but for the four locations mentioned previously. To obtain a generic corrective algorithm that can be applied to forecasts made for different areas with different orography and climate, the measurements and predictions for each site were treated as data from only one site to find the ANN parameters that improved forecasts in average.

Some parameters were predefined such as the functions used for pre-processing data and the performance function (mean squared error). The ANN type was defined as a fitting network with 3 layers, a hyperbolic tangent sigmoid as transfer function and Bayesian regulation backpropagation as training function. Data was grouped in different sets so that only days with similar predicted daily clearness indexes were used to train (80% of the data) and validate (20% of the data) the ANN. For training termination 20 validation checks were used. The data was divided into 3 categories according to the predicted daily clearness index (K_t): clear sky days ($K_t \geq 0.65$); partially cloudy days ($0.4 \leq K_t < 0.65$) and overcast days ($K_t < 0.4$). The common inputs were calculated solar radiation on top of the atmosphere as well as predicted GHI, visibility, cloud base height, total column water, total cloud cover, wind intensity, 2 meter air temperature, relative air humidity and total column ozone. Additionally, the ANN was improved by including the solar global radiation in clear sky conditions as calculated through the ASHRAE model [13], the hour, day and month for clear sky days and only the solar global radiation in clear sky conditions for overcast days.

The hourly differences between the absolute differences of predictions and measurements and simulations and measurements of GHI are then calculated so that this difference is positive if the ANN improves the forecasts and negative if not. A percentage of hours when the simulation results are equal or better (closer to the measurements) than the original predictions was also calculated. These parameters were used to find the ANN parameters that resulted in the best approximation to reality.

The deviation from the predicted daily clearness index of the day to simulate was made to vary from 0.005 to 0.15 and it was shown that the best simulations occurred for deviations of 0.145 for clear sky days and overcast days and 0.15 for partially cloudy days. The number of neurons in the hidden layer was chosen to range from 1 to 100 and it was shown that the best simulations occurred when using 27 neurons for overcast days, 30 for partially cloudy days and 58 for clear skies. These were the parameters defined for the corrective algorithm that allows for the correction of hourly GHI forecasts from ECMWF improving them by 22 kJ/m^2 on average and resulting in values closer to reality or equal to the predictions in 61,84% of the times.

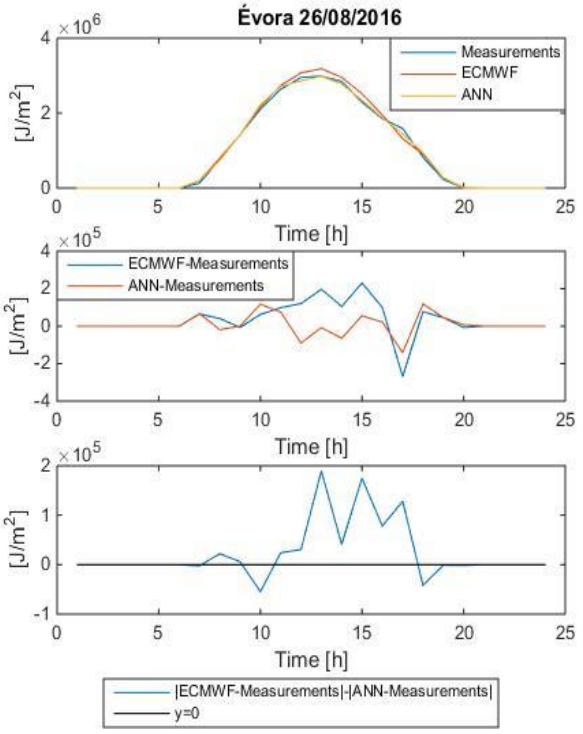

Fig. 5. Results of the usage of the ANN for correction of ECMWF's hourly GHI forecasts for 26 of August of 2016 in Évora.

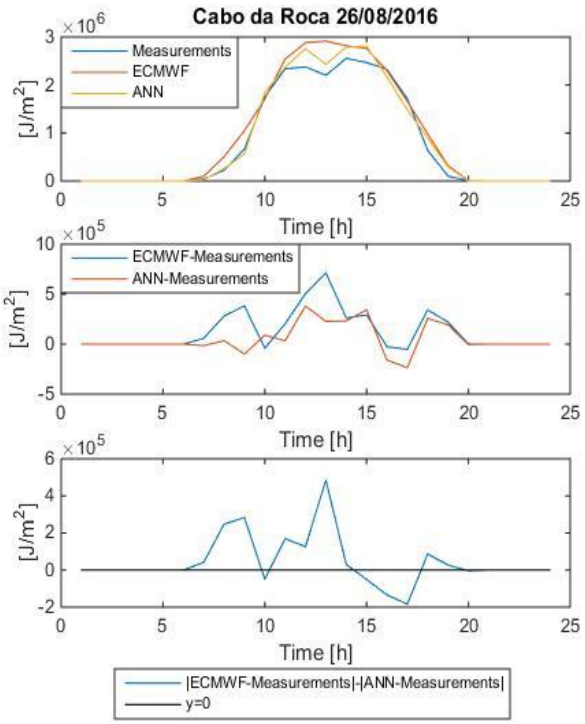

Fig. 6. Results of the usage of the ANN for correction of ECMWF's hourly GHI forecasts for 26 of August of 2016 in Cabo da Roca.

An example of the correction of predicted hourly values of GHI for all 4 sites of measurements was analyzed. Figures 5 and 6 show the results for Évora and Cabo da Roca respectively. In these figures, the graphic in the top shows the hourly GHI measured, forecasted by the ECMWF and simulated using the corrective algorithm. In Évora there is a smooth curve characteristic of a clear sky day while for Cabo da Roca there are signs of clouds. The middle graphic in the figures shows the differences between the hourly forecasts and measurements and between the hourly simulations made using the ANN and measurements of GHI. Ideally these differences would be null meaning that the forecasts and simulations would match the measurements, for this day the differences between simulations and measurements are usually closer to 0 (average of the hourly differences for all 4 sites of approximately 10 kJ/m^2) than the difference between forecasts and measurements (average of the hourly differences for all 4 sites of 49 kJ/m^2) meaning that in average the algorithm successfully corrected the hourly forecasts. This can also be seen in the bottom graphic of each figure that shows the differences between differences, where positive values mean that the simulations are closer to the measurements than the forecasts being the average value of 75170 J/m^2 for all 4 sites and being the simulations better or equal to the forecasts in 69.23% of the time.

CONCLUSION

In this paper, the influence of atmospheric and Sun-Earth geometry related variables on the differences between predictions and measurements of solar global radiation was analysed and an ANN algorithm was developed to correct predicted values of solar global radiation. It was shown that the differences associated to the forecasts would have a larger impact on the predicted conversion of energy when the clearness index is of 40% to 70% and for minimum values of zenith. The differences between predicted and measured values of solar global irradiation showed a relation with the predicted values of mean air temperature, relative air humidity and total water column. The algorithm developed based on ANN methodology allows the correction of hourly solar global radiation forecasts from ECMWF improving them by 22 kJ/m^2 in average and resulting in values closer to measurements used as reference or equal to the forecasts in 61,84% of the times. This algorithm is integrated in a more complete model, a global solar radiation and mean air temperature prediction algorithm that will be used in energy management in medium/low temperature solar thermal systems. It is expected that the integration of the algorithm in these types of models or models of other solar energy conversion units, will allow for a better management of renewable energy conversion and a better design and usage of conventional auxiliary systems.

REFERENCES

[1] M. Paulescu *et al.*, *Modeling Solar Radiation at the Earth Surface*. 2013.

[2] A. Culclasure, “Using Neural Networks to Provide Local Weather Forecasts”, *Electron. Theses Diss.*, 2013.

[3] B. Amrouche and X. Le, “Artificial neural network based daily local forecasting for global solar radiation”, *Appl. Energy*, **130**, 2014, pp. 333–341.

[4] C. Voyant *et al.*, “Machine learning methods for solar radiation forecasting : A review”, *Renew. Energy*, **105**, 2017, pp. 569–582.

[5] F. J. L. Lima *et al.*, “Forecast for surface solar irradiance at the Brazilian Northeastern region using NWP model and arti fi cial neural networks”, *Renew. Energy*, **87**, 2016, pp. 807–818.

[6] C. P. Sweeney *et al.*, “Reducing errors of wind speed forecasts by an optimal combination of post-processing methods”, *Meteorol. Appl.*, 2011.

[7] S. Dimopoulou *et al.*, “Forecasting of Photovoltaic Power at Hourly Intervals with Artificial Neural Networks under Fluctuating”, *Energies*, 2016, pp. 1–13.

[8] K. Abhishek *et al.*, “Weather forecasting model using Artificial Neural Network”, *Procedia Technol.*, **4**, 2012, pp. 311–318.

[9] P. Malik and B. Arora, “An Effective Weather Forecasting Using Neural Network”, *Int. J. Emerg. Eng. Res. Technol.*, **2**, 2014, pp. 209–212.

[10] E. Anderson, “User Guide for ECMWF forecast products. ECMWF.” 2015.

[11] S. Pereira *et al.*, “Spatial and temporal downscaling of solar global radiation and mean air temperature from weather forecast data - an introductory numerical study and validation”, in *Workshop On Earth Sciences 2016*, 2016, pp. 8–11.

[12] International Organization for Standardization [ISO], “ISO 9060:1990. Solar energy -- Specification and classification of instruments for measuring hemispherical solar and direct solar radiation”, p. 11, 1990.

[13] American Society of Heating Refrigerating and Air-Conditioning Engineers Inc., “ASHRAE Handbook of fundamentals,” 2005, pp. 1–845.

ACKNOWLEDGMENT

This work was carried out under the contract with the company Warmhole, lda for the development of a solar radiation forecast algorithm. The authors wish to acknowledge ECMWF and IPMA for the provision of data and the funding provided by the European Regional Development Fund, included in the COMPETE 2020 (Operational Program Competitiveness and Internationalization) through the ICT project (UID/GEO/ 04683/2013) with the reference POCI-01-0145-FEDER -007690, DNI-A (ALT20-03-0145-FEDER-000011) and ALOP (ALT20-03-0145-FEDER-000004) projects.